Journal of Structural Biology 176 (2011) 119–126

Contents lists available at ScienceDirect

Journal of Structural Biology

journal homepage: www.elsevier.com/locate/yjsbi

^{26}Mg labeling of the sea urchin regenerating spine: Insights into echinoderm biomineralization process

Przemysław Gorzelak [a], Jarosław Stolarski [a,*], Philippe Dubois [b], Christophe Kopp [c], Anders Meibom [c]

[a] Institute of Paleobiology, Polish Academy of Sciences, Laboratory of Biostructures and Biomineralization, Twarda 51/55, PL-00-818 Warsaw, Poland
[b] Université Libre de Bruxelles, Faculté des Sciences, Laboratoire de Biologie marine, CP 160/15, av., F.D. Roosevelt, 50 B-1050 Bruxelles, Belgium
[c] Muséum National d'Histoire Naturelle, Laboratoire de Minéralogie et Cosmochimie du Muséum (LMCM), UMR 7202, Case Postale 52 61, rue Buffon, 75005 Paris, France

ARTICLE INFO

Article history:
Received 18 May 2011
Received in revised form 6 July 2011
Accepted 16 July 2011
Available online 22 July 2011

Keywords:
Biomineralization
Sea urchin
Calcite
$CaCO_3$
^{26}Mg labeling
NanoSIMS
SEM

ABSTRACT

This paper reports the results of the first dynamic labeling experiment with regenerating spines of sea urchins *Paracentrotus lividus* using the stable isotope ^{26}Mg and NanoSIMS high-resolution isotopic imaging, which provide a direct information about the growth process. Growing spines were labeled twice (for 72 and 24 h, respectively) by increasing the abundance of ^{26}Mg in seawater. The incorporation of ^{26}Mg into the growing spines was subsequently imaged with the NanoSIMS ion microprobe. Stereom trabeculae initially grow as conical micro-spines, which form within less than 1 day. These micro-spines fuse together by lateral outgrowths and form a thin, open meshwork (inner stereom), which is subsequently reinforced by addition of layered thickening deposits (outer stereom). The (longitudinal) growth rate of the inner stereom is ca. 125 μm/day. A single (ca. 1 μm) thickening layer in the stereom trabeculae is deposited during 24 h. The thickening process is contemporaneous with the formation micro-spines and involves both longitudinal trabeculae and transverse bridges to a similar degree. Furthermore, the skeleton-forming cells remain active in the previously formed open stereom for at least 10 days, and do not migrate upwards until the end of the thickening process. The experimental capability presented here provides a new way to obtain detailed information about the skeleton formation of a multitude of marine, calcite producing organisms.

1. Introduction

Echinoderms form a unique skeleton composed of numerous plates (ossicles) that are secreted within syncytial membranes through a biologically controlled intracellular biomineralization process (e.g., Okazaki, 1960; Märkel, 1986). Each ossicle consists of a tridimensional meshwork made of magnesium calcite trabeculae (stereom) and of about 0.1% (w/w) organic components (the so-called intrastereomic organic matrix; "IOM"; see Weiner, 1985). Both mineral and organic materials are structured within individual stereom trabeculae in a form of alternate concentric layers (e.g., Dubois, 1991; Ameye et al., 1998). It has been argued that the basic mechanisms of biomineralization are identical within the entire phylum Echinodermata, as suggested by very similar structures, properties, morphogenesis and molecules involved in the skeletogenesis (Dubois and Chen, 1989).

Previous work on the stereom structure has documented six stereom types: rectilinear, laminar, galleried, labyrinthic, microperforate and fascicular, as well as four stereom layers: retiform, simple perforate, irregular perforate and imperforate (Smith, 1980). According to Dubois and Jangoux (1990) morphogenesis of all stereom types is basically the same. Most of available data on stereom growth come from regenerating spines of echinoids and asteroids (see e.g., Heatfield, 1971; Mischor, 1975; Dubois and Jangoux, 1990). According to these data, spine regeneration appears to be very similar to the original spine growth. Regeneration starts with a wound-healing phase during which the epidermis is reconstituted around the broken surface of the spine. Formation of new skeleton usually begins 3 days after breakage, below the healed epidermis, in the form of small conical projections (the so-called micro-spines) on the fractured surface of trabeculae. According to Politi et al. (2004), the very first deposits are made of amorphous calcium carbonate particles that seem to aggregate and subsequently crystallize into macroscopic single crystals of calcite (Yang et al., 2011). Initially, these micro-spines grow parallel to the longitudinal axis of the spine (which is also the *c*-crystallographic axis of calcite). Lateral branches are formed at regular intervals to connect neighboring micro-spines into a thin tri-dimensional fenestrated meshwork (the so-called open stereom). This thin meshwork subsequently thickens by secondary deposition of mineral on previously formed meshes (Heatfield, 1971; Mischor, 1975; Dubois and Ameye, 2001).

* Corresponding author. Fax: +48 22 620 62 25.
E-mail addresses: pgorzelak@twarda.pan.pl (P. Gorzelak), stolacy@twarda.pan.pl (J. Stolarski), phdubois@ulb.ac.be (P. Dubois), Kopp.christophe@hotmail.fr (C. Kopp), meibom@mnhn.fr (A. Meibom).

1047-8477/$ - see front matter © 2011 Elsevier Inc. All rights reserved.
doi:10.1016/j.jsb.2011.07.008

Such interpretations of the dynamics of stereom growth were based on comparisons of different spines removed from the echinoid body at different time-intervals. A more direct way to observe spine formation would be to dynamically label the spine during growth and subsequently observe the label incorporated into the formed structures at the nano/micrometer scale. Although different types of chemical markers (e.g., calcein) have been used to study skeleton formation of various organisms, including echinoderms, care has to be taken that such markers do not stress the organism and perturb the biomineralization processes under study (see Section 4). Furthermore, the spatial resolution provided by these markers is rather poor.

Recently, Houlbréque et al. (2009) presented a new method of labeling of scleractinian coral aragonite with elevated abundances of the stable isotope ^{86}Sr, which is a natural component of seawater. Subsequently, it has been documented that such labeling procedures do not stress the organism in any measurable way (Brahmi et al., 2010 submitted to JSB). Houlbréque et al. (2009) used the NanoSIMS ion microprobe to image the incorporation of the ^{86}Sr label with high spatial resolution. Because the concentration of Mg in calcite usually is higher than the concentration of Sr (Menadakis et al., 2007), it is advantageous to label with ^{26}Mg in calcitic structures, such as the skeleton of echinoids. In this paper we combine such ^{26}Mg labeling of the magnesium calcite skeleton of echinoids with NanoSIMS imaging of the resulting structures. The results reveal interesting aspects of the skeletal growth of echinoderms and the method is a broadly applicable tool to study the dynamics of biomineralization processes of a wide range of calcite-producing organisms.

2. Materials and methods

The ^{26}Mg experiments were conducted in the Laboratory of Marine Biology in Brussels (Faculté des Sciences, Université Libre de Bruxelles, Belgium) using young sea urchins *Paracentrotus lividus* (Lamarck), 32–35 mm in ambital diameter (Fig. 1A–C) obtained from the aquaculture facility in Luc-sur-Mer (English Channel, Normandy, France). The specimens were transported to Brussels and maintained for 2 weeks in an aerated, closed circuit aquarium, containing about 1000 l of natural seawater (Wimereux, Pas-de-Calais, France) under controlled and constant temperature (about 17 °C), salinity (32 psu), and pH conditions (about 8.0), similar to the conditions in the aquaculture facility. The experiment involved the following steps (see also Fig. 4): (1) Spine fracturing; (2) 3 days (72 h) recovery; (3) 1 day (24 h) simulated labeling experiment; (4) 3 days (72 h) ^{26}Mg labeling; (5) 3 days (72 h) recovery; (6) 1 day (24 h) ^{26}Mg labeling; (7) 3 days (72 h) recovery after which the experiment ended and the animals were sacrificed. The experimental steps are explained in more detail below.

Two specimens were prepared 4 days before the beginning of the labeling experiment by cutting distal portions of a few long primary spines, thereby starting the process of spine regeneration (Fig. 1D). Three days after cutting the spines, a 'simulated' labeling experiment was conducted to examine potential signs of stress. In this 'simulated' experiment, the sea urchins were incubated separately for 1 day in two 500 ml beakers containing 1 liter of artificial seawater obtained by mixing Milli Q water (Millipore) with Wiegandt sea-salt and a solution containing 288 mg dissolved MgO of normal isotopic composition.

MgO is a highly refractory oxide and highly insoluble in seawater. In order to bring MgO into solution a strong acid is needed, which naturally results in a very low pH of the solution. The pH had to be brought up to the natural value around pH 8 before the MgO solution can be added to the seawater. This was achieved in the following way. First, about 7.4 ml of 6.25% HCl was added drop by drop to

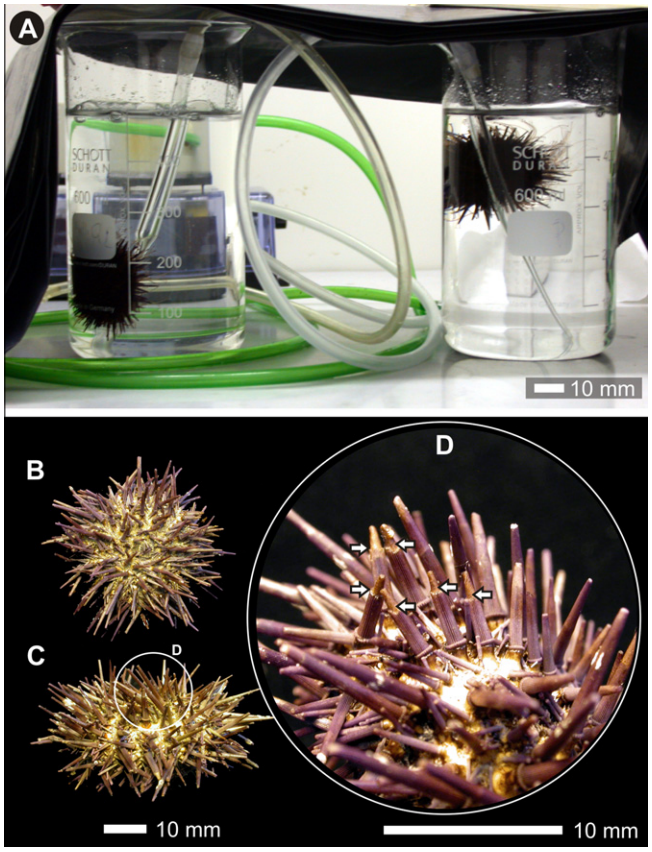

Fig.1. (A) Two specimens of sea urchins *Paracentrotus lividus* in beakers with fully expanded podia during labeling with ^{26}Mg enriched artificial seawater. (B) Aboral and (C) lateral views of dissected specimens with enlargement (D) of the test fragment with regenerated fragments of spines (arrows).

288 mg of MgO. The resulting solution was equilibrated for about 1 h to insure complete dissolution of the oxide. Second, about 300 mg $NaHCO_3$ was slowly added in order to bring up the pH of the solution to the natural level. This MgO solution was then added to 1 liter of artificial seawater under mixing for about 2 h. The pH of this final solution was monitored to insure that large departures from the natural pH did not occur (see Appendix A). The sea urchins were transferred to this solution after its equilibration.

During this simulated test, the sea urchin podia actively moved and there were no signs that the animals were stressed. Note that specimens of echinoids (*Eucidaris tribuloides* (Lamarck)) have previously been grown in artificial seawater with increased Mg^{2+}/Ca^{2+} ratio (i.e. 6.7), without producing signs of anomalous metabolic effects or general stress (Ries, 2004).

Having observed that the sea urchins did not show signs of stress during handling and labeling procedures, the two specimens were incubated in artificial seawater labeled with $^{26}Mg^{2+}$ by dissolving 288 mg/l ^{26}MgO powder (commercially available from the Oak Ridge National Laboratory, USA) in a manner similar to that described above. This addition of ^{26}Mg to the artificial sea-water was calculated to produce an increase in the ^{26}Mg concentration by a factor of 2.5 and corresponded to an increase in the total Mg^{2+}concentration of only 16.5%; i.e. the calculated Mg^{2+}/Ca^{2+} ratio was only slightly increased from about 5.2 to about 6, and the pH of the water was not affected (c.f. Table 1). This addition of ^{26}Mg is unlikely to perturb the organism and have detrimental effects on the biomineralization processes.

During labeling events, each sea urchin was incubated in 500 ml beakers, equipped with aquarium air pump and covered by foil (Fig. 1A). In the first labeling event, both specimens were incubated

Table 1
Conditions in beakers during experiment. Temperature, salinity and pH of the ^{26}Mg-labeled artificial seawater were kept similar to the natural habitat of the sea urchins. SD = standard deviation.

Date	Hour	Beaker 1			Beaker 2		
		pH	Temperature (°C)	Salinity (psu)	pH	Temperature (°C)	Salinity (psu)
First 3-day labeling							
2010-06-22	6:00 PM	8.27	17.5	31.8	8.22	17.5	31.8
2010-06-23	9:00 AM	7.98	17.4	32.1	7.96	17.5	31.9
	2:00 PM	7.93	17.5	32.2	7.88	17.4	31.8
	6:00 PM	7.78	17.4	32.1	7.78	17.3	32
2010-06-24	9:00 AM	8.1	17.2	32.2	8.12	17.6	32.1
	2:00 PM	7.95	17.5	32.2	7.97	17.7	32.1
	6:00 PM	7.93	17.4	32.3	7.91	17.3	32.2
2010-06-25	9:00 AM	8.16	17.6	32.4	8.15	17.6	32.1
	2:00 PM	7.93	17.2	32.4	7.87	17.3	32.3
	6:00 PM	7.84	17.3	32.5	7.83	17.3	32.3
Second 1-day labeling							
2010-06-28	6:00 PM	7.74	17.5	32.3	7.7	17.3	32.2
2010-06-29	9:00 AM	8.12	17.5	32.3	8.18	17.3	32
	2:00 PM	8.01	17.3	32.3	7.89	17.3	32.1
	6:00 PM	8.03	17.6	32.5	7.93	17.6	32.3
SD		0.147	0.131	0.183	0.156	0.149	0.170
Range		7.74–8.27	17.2–17.6	31.8–32.5	7.7–8.22	17.3–17.7	31.8–32.3
Mean		7.98	17.42	32.26	7.96	17.43	32.09

for a total of 72 h. During the experiment, temperature, salinity and pH were measured three times per day using a WTW Multi 340i multi-meter equipped with a conductivity cell, pH electrode and integrated temperature sensor (Table 1). The tendency towards a salinity increase of artificial seawater due to evaporation was counteracted by the gradual addition of Milli Q water (Millipore). The weak tendency for a drop in the pH was compensated by small additions of $NaHCO_3$.

Alkalinity values, measured by a potentiometric titration with HCl 0.1 M using a Titrino 718 STAT Metrohm (Switzerland), and calculated using the Gran function (Gran, 1952), fell in the range 4.2–3.9 mmol/kg at the beginning and 3.9–3.8 mmol/kg at the end of the experiment for both beakers. After the incubation, sea urchins were returned to normal conditions in the aerated, closed circuit aquarium, containing about 1000 l of natural seawater with natural isotopic abundances of Mg^{2+}.

After 3 days, a 1-day labeling procedure was carried out using the same ^{26}Mg-enriched seawater, which had been filtered (GSWP Millipore filters with 0.22 μm pore size) and kept refrigerated between the two labeling events. As was also the case during the first labeling event, throughout the second labeling experiment, the two sea urchins actively moved and produced new skeleton, suggesting that they did not suffer stress. After the last labeling event, specimens were returned to normal aquarium conditions for 3 days before the experiment was terminated.

At the end, sea urchins were dissected and the inner organs were separated from the body wall. The skeletons were then rinsed using Milli Q water and dried at 50 °C for 48 h. The associated soft tissues were removed by soaking in 5% sodium hypochlorite for 24 h at room temperature. Regenerated spines were mounted in epoxy, polished down to a 0.25 mm finish with diamond suspensions, gold-coated and imaged with the NanoSIMS ion microprobe at the Muséum National d'Histoire Naturelle in Paris.

NanoSIMS analyses were carried out with a primary beam of negatively charged oxygen focused to a spot-size of ~200 nm on the surface of the sample. The secondary ions $^{44}Ca^+$ and $^{26}Mg^+$ were detected in multi-collector mode with electron multipliers at a mass resolving power of ~5000, which allows all potentially problematic mass-interferences to be resolved (Meibom et al., 2004, 2008). Images of 256 by 256 pixels were obtained by rastering the primary beam across a pre-sputtered surface with a pixel dwelling time of 10 ms. Following NanoSIMS imaging, the remaining gold coating was removed and the samples lightly etched in Mutvei's solution following described procedures (Schöne et al., 2005). Similar effects were also obtained by ca. 20 s etching in 0.1% formic acid solution, following Stolarski (2003). This brought out the ultra-structural details of the skeleton. The samples were then recoated with gold and observed in a Phillips XL30 scanning electron microscope (SEM).

3. Results

The spines of *P. lividus* are similar to those of other sea urchins. They consist externally of a proximal basal portion (a base), a milled ring and a distal, tapering shaft (Fig. 2A). The base, which is articulated on a tubercle of the test in a ball-and socket joint, is composed of meshwork stereom, whereas the shaft is made of radially arranged septa of compact imperforate stereom that are joined by transverse bridges. The center of the spine is filled with classical meshwork stereom.

The data obtained by labeling experiment are summarized in Figs. 2–4. The two labeling events are clearly visible in the $^{26}Mg^+/^{44}Ca^+$ NanoSIMS maps and provide detailed information about growth dynamics of regenerating spine and about morphogenesis of stereom meshwork and individual stereom trabecula (Fig. 5).

3.1. Dynamics of growth of regenerating spine

Judging from Fig. 2, the growth of regenerating spine was probably initiated about 3 or 4 days after fracture because labeled stereom is visible close to the fractured surface (Fig. 2). After the onset of spine regeneration, the growth rate rapidly became relatively constant (Fig. 4). During the first labeling event, about 465 μm of new spine were formed (Figs. 2B,C and 4), equivalent to a mean longitudinal growth rate about 155 μm/day. The growth rate did not change significantly thereafter. During the 3 days between two labeling events the total longitudinal growth was about 380 μm, which corresponds to a mean growth rate about 127 μm/day; Fig. 4). In the second (1-day) labeling event, about 110 μm of new spine grew (Figs. 2D and 4). After the second labeling event, in the 3 days before the experiment was terminated, about 375 μm of new spine were formed (Figs. 2C and 4), equivalent to a mean

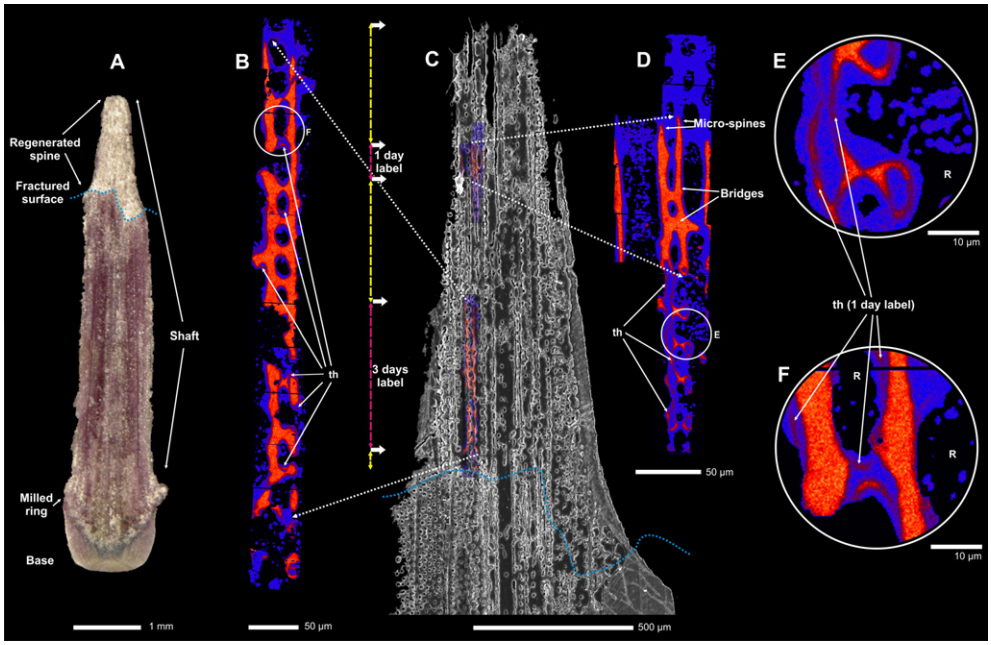

Fig.2. (A) Lateral view of investigated spine of *P. lividus* with regenerated fragment of apical part. (C) Lateral view (Scanning Electron Microscope) of a polished and Au-coated section of spine combined with NanoSIMS images showing two labeling events (dotted arrows show position of NanoSIMS images enlarged in B, D). Etching and SEM observations were performed after the NanoSIMS imaging. (B) NanoSIMS image of the $^{26}Mg/^{44}Ca$ distribution in labeled skeleton during first (3-day) labeling event. (D) NanoSIMS image of the $^{26}Mg/^{44}Ca$ distribution in labeled skeleton during second 1-day labeling event. Blue regions indicate growth in normal (i.e. unlabeled) artificial seawater with normal $^{26}Mg/^{44}Ca$ ratio. Red–yellow regions indicate enhanced $^{26}Mg/^{44}Ca$ ratio due to the ^{26}Mg labeling. (E, F) Enlargements of the stereom showing 1-day thickening process ("th" and arrows) during the second labeling event on the previously formed skeleton. "R" marks resin-filled pores.

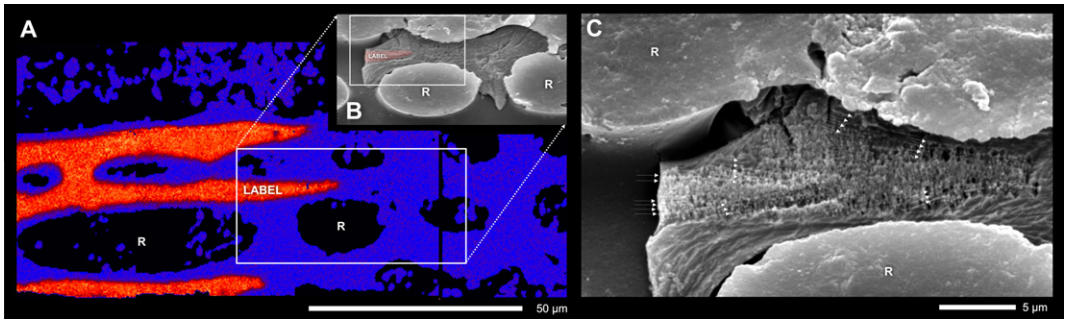

Fig.3. (A) Fragment of NanoSIMS image of the $^{26}Mg/^{44}Ca$ distribution in labeled skeleton during second (1-day) labeling event superimposed on SEM micrograph of the slightly etched surface of the skeleton (B,C) exhibiting the concentric banding structure (arrows). Etching and SEM were performed after the NanoSIMS imaging. Blue regions indicate growth in normal (i.e. unlabeled) artificial seawater with normal $^{26}Mg/^{44}Ca$ ratio. Red–yellow regions indicate enhanced $^{26}Mg/^{44}Ca$ ratio due to the ^{26}Mg labeling. "R" marks resin-filled pores which are at the forefront due to etching (B, C). (For interpretation of the references in color in this figure legend, the reader is referred to the web version of this article.)

longitudinal growth rate of about 125 µm/day, respectively. Thus, the longitudinal growth-rate was relatively constant for the duration of the experiment. The absence of a growth-rate difference during and between labeling events indicates that the animal was not in any way stressed by the ^{26}Mg-labeling procedures (Fig. 4).

3.2. Morphogenesis of stereom meshwork and individual stereom trabecula

As illustrated in Figs. 2B,D and 3A,B the new skeleton first grows as minute, conical micro-spines that are oriented parallel to the longitudinal axis of the spine. These micro-spines are elongated (up to about 60 µm) and rather thin (about 3–4.5 µm in diameter near their base) and they have pointed or rounded tips. Individual micro-spine grows apically spaced by about 20–30 µm. Lateral growth takes place allowing adjacent micro-spines to join by forming a horizontal 'bridge' (Fig. 2D). This process is very fast and seems to occur several times per day (during the 3 days experiment we observed about 11 such bridges, suggesting a rate of about 3–4 per day) (Fig. 2B,D). The result is a three-dimensional fenestrated meshwork, with several meshes visible from the base to the top composed of thin (about 3–5 µm in diameter) trabeculae; this is the structure referred to as the open stereom. While new trabeculae form, the older trabeculae already connected in a thin meshwork, thicken simultaneously and very slowly with an approximate rate about 1 µm/day (Fig. 2B–F). This thickening process includes both micro-spines and bridges (e.g., Fig. 2B–F). After 14 days, the thickening trabeculae at the base of the fractured surface are about twice as thick as the initial micro-spines.

As shown in Figs. 2 and 3, ^{26}Mg labeled stereom is easily distinguished from the non-labeled skeleton regions. The concentric structure of stereom trabeculae that is composed of minute-scale

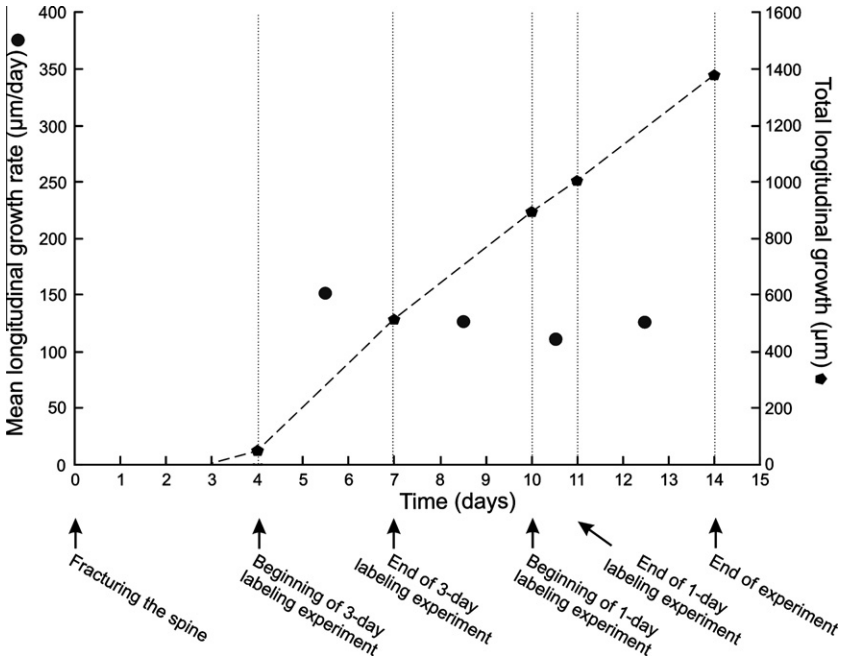

Fig.4. Plot showing total longitudinal growth and mean longitudinal growth rates of investigated skeleton during regeneration of fractured spine of *P. lividus*.

layers (Fig. 3B–C) does not correspond well with the specific ^{26}Mg distribution, as might have been expected from a thin secondary thickening layer (Fig. 2B,D–F) that was formed within the second 1-day labeling event. At least in some regions, its thickness (0.5–1.5 µm) is similar to the thickness of some of the nano-layers revealed after etching the stereom surface (compare Figs. 1.5–7 in Dubois and Jangoux, 1990; Figs. 3–6 in Dubois, 1991, see also Figs. 3C and 6).

4. Discussion

To date, antibiotic tetracycline and calcein have been used to study different aspects of skeletal growth in sea urchins (for review see Ebert, 2006). Both of these markers bind to Ca^{2+} and are incorporated into the carbonate skeletons during calcification, and can be visualized under ultraviolet illumination, where tetracycline fluoresces yellow and calcein fluoresces green. However, knowl-

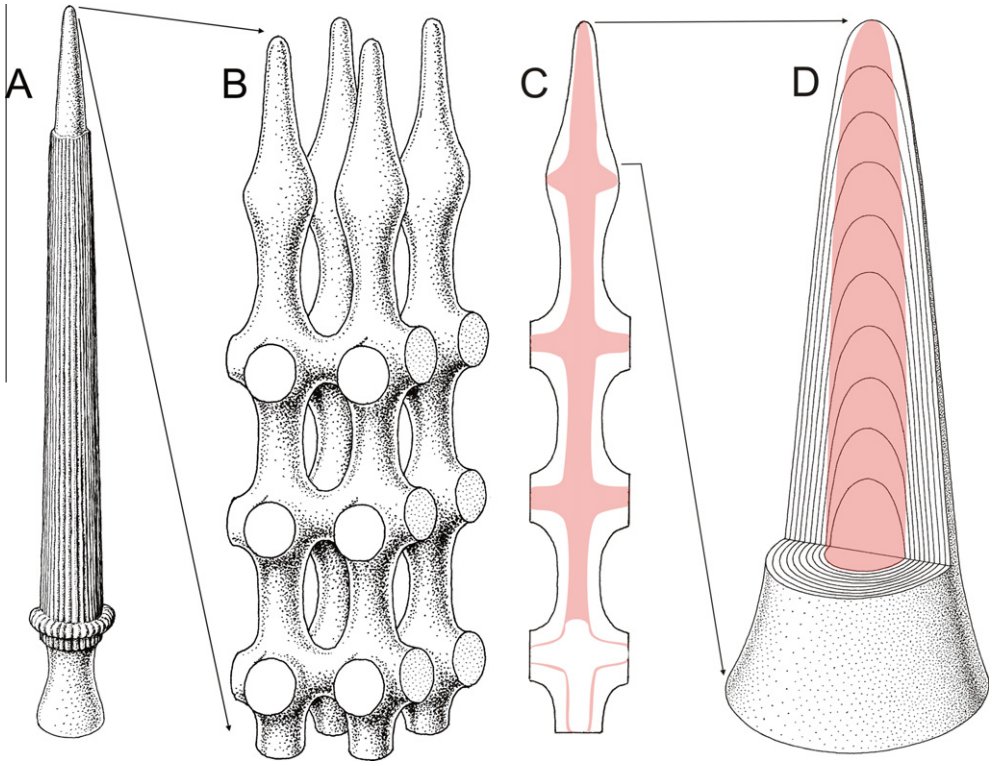

Fig.5. Model of regenerating echinoid spine (A), composed of stereom meshwork (B). Orange regions (C, D) show distribution of isotope label (^{26}Mg) as observed in the experiment (example taken from 1-day labeling, see Fig. 2D); thin, labeled thickening layer (bottom in C), is continuous with massive labeling indicating that skeleton-forming cells are still active in the previously formed open stereom and do not migrate upwards until the end of the thickening process (For interpretation of the references to colour in this figure legend, the reader is referred to the web version of this article.).

edge of how these chemicals can influence echinoderm physiology is limited. For example, sea urchins injected with large volumes of tetracycline often developed flaccid tube feet and were unable to attach to substrate (Ebert, 2006). Calcein that is commonly used a chemical marker, has a high affinity for Ca^{2+} and low affinity for Mg^{2+} (Chiu and Haynes, 1977). Therefore, it may lead to changes in cell functions and possibly perturb the biomineralization process. For example, it has been shown that calcein does interfere with the growth of marine mollusks (Thébault et al., 2006). Clearly negative effects of calcein have been also observed in fish, which had decreased survival-rate after addition of even low concentrations of calcein (Brooks et al., 1994; Bumguardner and King, 1996; Gelsleichter et al., 1997). In sea urchins, Russell and Urbaniak (2004) reported a short-term effect (1 week) on growth rate but no effect at longer term (10 weeks). Apart from these chemicals, there are a few other stains (such as alizarin red) that have been used to study skeletal formation of various organisms, including echinoderms. It is generally accepted, however, that alizarin may also have a negative impact on physiology of some marine organisms, such as corals (e.g., Dodge et al., 1984).

The examples above show that various chemicals may induce stress on organisms and consequently disturb micro/nano-scale growth of the skeleton. Furthermore, their resolution is limited to the optical microscope level. An advantage of using the stable isotope ^{26}Mg as a marker is that it is a natural component of seawater that is present in the calcite skeleton in a concentration high enough that it can be easily imaged using NanoSIMS ion microprobe with a sub-micrometer scale lateral resolution.

This new method provided insights into various aspects of echinoderm biomineralization process. The ^{26}Mg-labeling experiment shows that a mean longitudinal growth rate for *P. lividus* was about 130 μm/day (Fig. 4). This growth rate is comparable to those observed in *Strongylocentrotus purpuratus* (Stimpson) (160 μm/day) and *Arbacia punctulata* (Lamarck) (260 μm/day) (for details see Heatfield, 1971). Although our observations are generally consistent with previous reports on the early stages of the stereom growth (Heatfield, 1971; Mischor, 1975), they also provide new and much more detailed information on stereom formation. So far, the precise timing of micro-spine formation has not been known. This study shows that individual micro-spines can grow very fast, within less than 1 day. The fusion of adjoining micro-spines through lateral process can also be accomplished on time scales much shorter that 1 day and in fact happened 3–4 times per day under the conditions studied here (Fig. 2B).

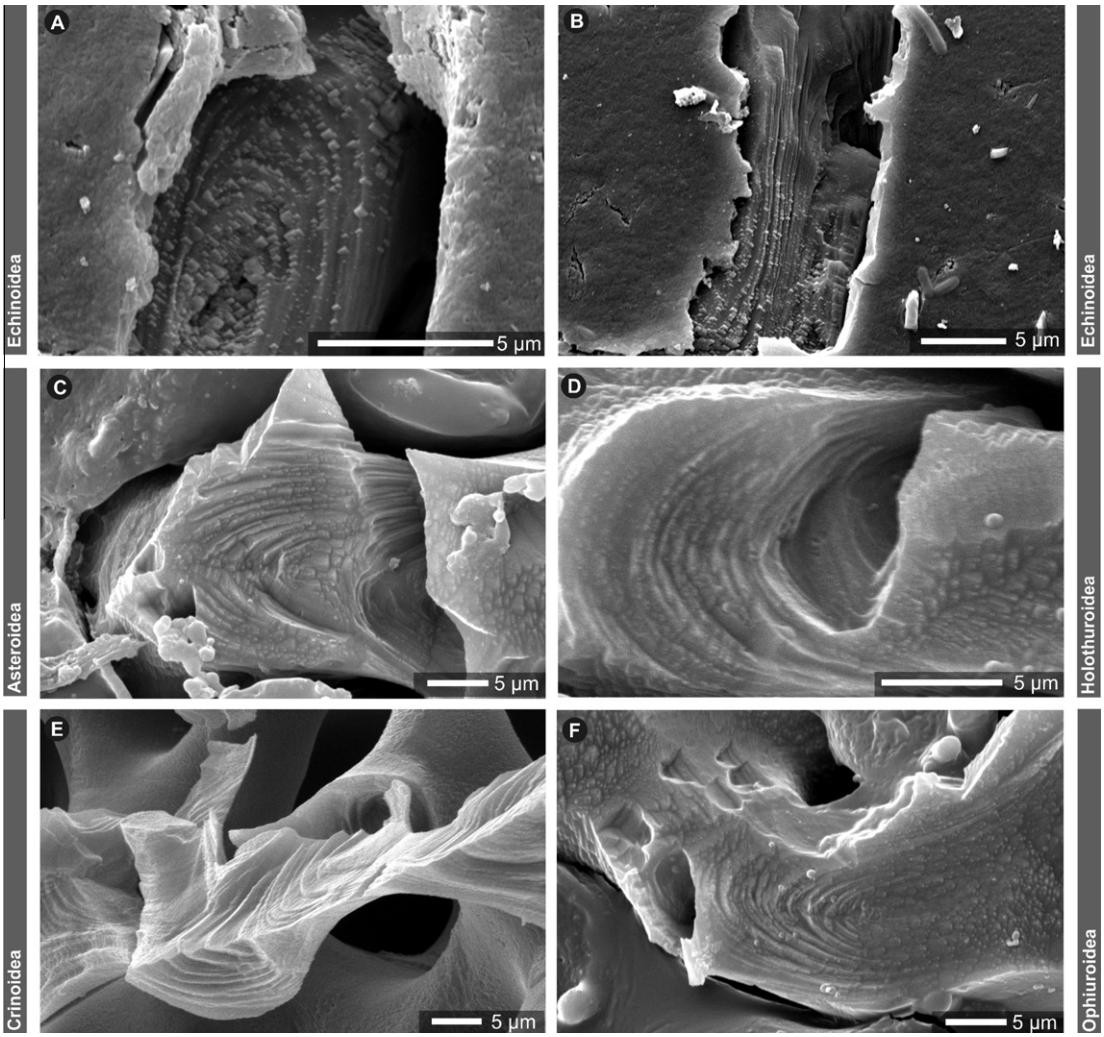

Fig.6. SEM micrographs of stereom fragments representating of five extant classes of echinoderms. Concentric lamination revealed by slight acidic etching on polished or fractured surfaces parallel to the longitudinal axis of the stereom bars. (A, B) Echinoid *P. lividus* (Normandy, France); spine, inner (A) and outer (B) zone of the stereom bar. (C) Asteroid *Asterias rubens* (North Atlantic Ocean, Gulf of Maine); inferomarginal spine. (D) Holothuroid *Psolus phantapus* (North Sea, precise location unknown); radial piece of calcareous ring. (E) Crinoid *Neocrinus decorus* (North Atlantic Ocean, Grand Bahama Island); columnal. (F) Ophiuroid *Ophiocoma insularia* (central Pacific Ocean, Paia Bay, Maui Island, Hawaii); arm spine.

Calculations of the growth rate of trabeculae were made considering that ^{26}Mg is deposited during the labeling periods (3 days and 1 day). Although it cannot be completely ruled out that some ^{26}Mg is stored in the soft tissues for some time (see Lewis et al., 1990 for such delayed incorporation of ^{45}Ca) the following observations suggest that transfer of ^{26}Mg to the skeleton is very fast: (i) the ^{26}Mg enrichment is a sharp feature and there is no residual or delayed labeling skeleton after the end of a labeling event, (ii) labeled skeleton is present very close to the fractured surface, (iii) there are no growth-rate differences during and between labeling events (with normal Mg/Ca ratio).

Thickening of the trabeculae occurs simultaneously with formation of new open meshwork of thin micro-spines connected by bridges. While new trabeculae grow, older trabeculae thicken simultaneously but very slowly (with an approximate rate about 1 μm/day). This implies that the skeleton-forming cells are still active in the previously formed open stereom and do not migrate upwards until the end of the thickening process. Intriguingly, TEM histological studies of the regenerating sea urchin spines (*S. purpuratus*) suggested that active sclerocytes (skeleton secreting cells) were present only at the tips and adjacent proximal portions of the longitudinally oriented microspines and not in deeper parts of the stereom (Heatfield and Travis, 1975). Our conclusions provide thus a stimulus for modern ultrastructural studies that would allow visualization of rapid cellular processes.

Our experiment also provides insights into timing of nano/micro-scale growth increments of the trabecular bar, the smallest structural element of the stereom. Trabecular bars, when selectively etched, reveal concentric banding structure, interpreted as alternation of mineral and organic-enriched layers (Dubois and Jangoux, 1990: Figs. 1.5–7; Dubois, 1991: Figs. 3–6, see also Figs. 3 and 6). The time span required for formation of such layers, which are usually less than 1 μm thick, has not hitherto been estimated. Although individual micro-bands were not clearly recognized within continuously ^{26}Mg-labeled skeleton (c.f. 1-day and 3-day labeling events in Figs. 2 and 3A,B), a thin secondary thickening layer, continuous with the 1-day ^{26}Mg-labeled micro-spines has a thickness similar to the layers revealed after etching the surface (Fig. 2D,E). This indicates that the timescale of formation of a single thickening layer on the trabeculae is on the order of 1 day.

From the results discussed above a highly dynamic growth process becomes apparent in which different parts of the skeleton are formed contemporaneously, but at very different rates. The longitudinal growth-rate of the inner part of trabecula is about 125 μm/day (extension rate of entire spine), which is equivalent to ca. 5 μm per hour (or 1 μm per 12 min). Individual layers in the thickening deposits form on times scale of about 1 μm per day. During our experiment it was not possible to visualize individual inner and outer stereom layers that are formed simultaneously (but at different growth rate) and for this purpose further, shorter (minutes to hours) labeling experiments are planned. Planned experiments will also address the issue of relationship between mineral phases during inner vs. outer stereom growth, as the amorphous calcium carbonate (ACC) was detected in microspines (inner stereom) of *P. lividus* sea urchin (Politi et al., 2004).

The layered structure of skeleton similar to that in sea urchin spine stereom is universal among representatives of all echinoderm classes (Fig. 6). In that respect, the stereom formation seems also to be analogous with layered structures of calcareous skeleton of scleractinian corals (Stolarski, 2003; Brahmi et al., 2010) or calcareous sponge spicules (Kopp et al., 2011) suggesting some common regulatory mechanisms. In all such instances, different cell types and/or cells of different metabolic/calcification activity are invoked to explain differences in growth dynamics between the skeletal regions. Nonetheless, only a limited number of studies (often indirectly) document such cellular/metabolic differences. In scleractinian corals, Le Tissier (1991) described two morphologically distinct cellular domains of the basal ectoderm that overlies different skeletal regions: (1) thin, with highly interdigitated lateral cell borders and prominent intracellular spaces in places of active skeletal deposition and (2) thick, without interdigitated lateral cell borders in places of less active skeleton deposition. Furthermore, two types of proteins intimately associated with the mineral phase of coral skeleton are involved in the deposition of structurally different mineral components: Galaxins are involved in controlling the fiber-like aragonite, and Amgalaxin-like molecules are associated with granular calcification (Reyes-Bermudez et al., 2009). Although functional links between different cell types (or/and their metabolism), secreted proteins, and their effects on skeletal structure have not been established yet in corals, their existence can be envisaged based on current biomineralization models (Addadi and Weiner, 1992; Wilt et al., 2003; Killian and Wilt, 2008). In calcareous sponges, different growth dynamics of spicule correspond to a spatial heterogeneity in cell type or activity (apical cell forming a primary nucleation site and a thickener cell spatially constraining lateral growth (Aizenberg et al., 1996; Ilan et al., 1996). Ameye et al. (2001) have shown that within stereom trabeculae of sea urchin *P. lividus*, organic matrix proteinaceous components are localized within different sub-regions of the spine skeleton: *N*-glycoproteins are associated with the inner core of stereom bar, whereas *O*-glycoproteins localized in outer surface of trabeculae, where skeletal growth is largely inhibited by comparison. Furthermore, Aizenberg et al. (1997) reported that the crystal texture differs between the meshwork stereom and the compact septa. Based on those examples, it can be suggested that echinoid spine formation involves different cellular activities and different types of organic components for the formation of different parts of the stereom, such as the inner and outer (thickening layers) stereom for which growth rates differ by more than a factor of 100.

5. Conclusions

The ^{26}Mg-labeling experiment showed that this stable isotope can successfully be used to precisely determine the site of carbonate deposition. The morphogenesis of stereom meshwork was found to be complex process of the initial, fast growth of thin open meshwork and simultaneous, slow thickening process. This new method of labeling with stable isotope ^{26}Mg that is a natural skeletal component open up new possibilities for investigating skeletal growth of other marine organisms that elaborate calcite skeletons.

Acknowledgments

We would like to thank: Mathieu Bauwens, Stéphanie Bonnet, Ana Dos Ramos Catarino, Marie Collard, Julie Hermans and Saloua M'Zoudi (all from Universite Libre de Bruxelles, Faculté des Sciences, Laboratoire de Biologie Marine, Bruxelles, Belgium) for technical assistance during the experiments. Special thanks are also due to: Tomasz K. Baumiller (Department of Geological Sciences, Univeristy of Michigan), Frederick H. C. Hotchkiss (The Marine and Paleobiological Research Institute, Massachusetts), and Grzegorz Niedźwiedzki (Department of Paleobiology and Evolution, Faculty of Biology, Warsaw University) for providing the specimens of crinoids, asteroids, ophiuroids and holothuroids. The National NanoSIMS facility at the Muséum National d'Histoire Naturelle was established by funds from the CNRS, Région Île de France, Ministère délégué à l'Enseignement supérieur et à la Recherche, and the Muséum itself. Financial support was provided by the Polish Ministry of Science and Higher Education through Grant N307-015733 to J. Stolarski, by the European Research Council through Advanced Grant 246749 (BIOCARB) to A. Meibom and by the Na-

tional Fund for Scientific Research (NFSR, Belgium), Contract No. 2.4532.07 to PhD (Senior Research Associate of the NFSR, Belgium). P. Gorzelak also thank the Foundation for Polish Science for financial support. We would like to thank the two anonymous referees for providing us with constructive comments and suggestions.

Appendix A

Preparation of solution with ^{26}MgO at 288 mg/L (~173.4 mg/L ^{26}Mg; an increase on the ^{26}Mg concentration by a factor of ~2.5).

(1) Add 7.4 ml 6.25% HCl to 288 mg ^{26}MgO; let this volume equilibrate for ca. 1 h.
(2) Add about 300 mg $NaHCO_3$ very slowly (the amount of added $NaHCO_3$ depends on the primary pH of artificial seawater; if it is about 8 you need to add more $NaHCO_3$).
(3) Add the volume (^{26}MgO dissolved in HCl and buffered by $NaHCO_3$) to 1 liter artificial seawater; mix using the electromagnetic stirrer for about 2 h).

Remark: add slowly the volume of HCl (drop by drop) as well as $NaHCO_3$ in order to avoid an important effervescence reaction and risk to loose some Mg.

References

Addadi, L., Weiner, S., 1992. Control and design principles in biological mineralization. Angew. Chem. Int. Ed. Engl. 31, 153–169.
Aizenberg, J., Ilan, M., Weiner, S., Addadi, L., 1996. Intracrystalline macromolecules are involved in the morphogenesis of calcitic sponge spicules. Connect. Tissue Res. 34, 255–261.
Aizenberg, J., Hanson, J., Koetzle, T.F., Weiner, S., Addadi, L., 1997. Control of macromolecule distribution within synthetic and biogenic single calcite crystals. J. Am. Chem. Soc. 119, 881–886.
Ameye, L., Compère, Ph., Dille, J., Dubois, Ph., 1998. Ultrastructure and cytochemistry of the early calcification site and of its mineralization organic matrix in *Paracentrotus lividus* (Echinodermata: Echinoidea). Histochem. Cell Biol. 110, 285–294.
Ameye, L., De Becker, G., Killian, C., Wilt, F., Kemps, R., et al., 2001. Proteins and saccharides of the sea urchin organic matrix of mineralization: characterization and localization in the spine skeleton. J. Struct. Biol. 134, 56–66.
Brahmi, C., Meibom, A., Smith, D.C., Stolarski, J., Auzoux-Bordenave, S., et al., 2010. Skeletal growth, ultrastructure and composition of the azooxanthellate scleractinian coral *Balanophyllia regia*. Coral Reefs 29, 175–189. doi:10.1007/s00338-009-0557-x.
Brooks, R.C., Heidinger, R.C., Kohler, C.C., 1994. Mass-marking otoliths of larval and juvenile walleyes by immersion in oxytetracycline, calcein, or calcein blue. N. Am. J. Fish. Manage 14, 143–150.
Bumguardner, B.W., King, T.L., 1996. Toxicity of oxytetracycline and calcein to juvenile striped bass. Trans. Am. Fish. Soc. 125, 143–145.
Chiu, V., Haynes, D.H., 1977. High and low affinity Ca^{2+} binding to the sarcoplasmic reticulum: use of a high-affinity flourescent calcium indicator. Biophys. J. 8, 3–22.
Dodge, R.E., Wyers, S.C., Frith, H.R., Knap, A.H., Smith, S.R., et al., 1984. Coral calcification rates by the buoyant weight technique: Effects of alizarin staining. J. Exp. Mar. Biol. Ecol. 75, 217–232.
Dubois, Ph., 1991. Morphological evidence of coherent organic material within the stereom of postmetamorphic echinoderms. In: Suga, S., Nakahara, H. (Eds.), Mechanisms and Phylogeny of Mineralization in biological Systems. Springer–Verlag, Tokyo, pp. 41–45.
Dubois, Ph., Ameye, L., 2001. Regeneration of spines and pedicellariae in echinoderms: a review. Microsc. Res. Tech. 55, 427–437.
Dubois, Ph., Chen, C.P., 1989. Calcification in echinoderms. Echinoderm Studies 3, 109–178.
Dubois, Ph., Jangoux, M., 1990. Stereom morphogenesis and differentiation during regeneration of fractured adambulacral spines of *Asterias rubens* (Echinodermata, Asteroidea). Zoomorphology 109, 263–272.
Ebert, T.A., 2006. Growth and survival of postsettelement sea urchins. In: Lawrence, J.M. (Ed.), Edible Sea Urchins: Biology and Ecology. Elsevier, Amsterdam, pp. 95–134.
Gelsleichter, J., Cortes, E., Manire, C.A., Hueter, R.E., Musick, J.A., 1997. Use of calcein as a fluorescent marker for elasmobranch vertebral cartilage. Trans. Am. Fish. Soc. 126 (5), 862–865.
Gran, G., 1952. Determination of the equivalence point in potentiometric titrages-Part II. Analyst 77, 661–671.
Heatfield, B.M., 1971. Growth of the calcareous skeleton during regeneration of spines of the sea urchin *Strongylocentrotus purpuratus* (Stimpson); a light and scanning electron microscope study. J. Morphol. 134, 57–90.
Heatfield, B.M., Travis, D.F., 1975. Ultrastructural studies of regenerating spines of the sea urchin *Strongylocentrotus purpuratus* I. Cell types without spherules. J. Morphol. 145, 13–49.
Houlbréque, F., Meibom, A., Cuif, J.-P., Stolarski, J., Marrocchi, Y., et al., 2009. Strontium-86 labeling experiments show spatially heterogeneous skeletal formation in the scleractinian coral *Porites porites*. Geophys. Res. Lett. 36, L04604. doi:10.1029/2008GL036782.
Ilan, M., Aizenberg, J., Gilor, O., 1996. Dynamics and growth patterns of calcareous sponge spicules. Proc. R. Soc. Lond. 263, 133–139.
Killian, C.E., Wilt, F.H., 2008. Molecular aspects of biomineralization of the echinoderm endoskeleton. Chem. Rev. 108, 4463–4474.
Kopp, C., Meibom, A., Beyssac, O., Stolarski, J., Djediat, S., et al., 2011. Calcareous sponge biomineralization: ultrastructural and compositional heterogeneity of spicules in *Leuconia johnstoni* Carter 1871. J. Struct. Biol. 173, 99–109. doi:10.1016/j.jsb.2010.07.006.
Lewis, C.A., Ebert, T.A., Boren, M.E., 1990. Allocation of ^{45}calcium to body components of starved and fed purple sea urchins (*Strongylocentrorus purpuratus*). Mar. Biol. 105, 213–222.
Märkel, K., 1986. Ultrastructural investigation of matrix-mediated biomineralization in echinoids (Echinodermata, Echinoidea). Zoomorphology 106, 232–243.
Menadakis, M., Maroulis, G., Koutsoukos, P.G., 2007. A quantum chemical study of doped $CaCO_3$ (calcite). Comp. Mater. Sci. 38, 522–525.
Meibom, A., Cuif, J.-P., Hillion, F., Constantz, B.R., Juillet-Leclerc, A., et al., 2004. Distribution of magnesium in coral skeleton. Geophys. Res. Lett. 31. doi:10.1029/2004GL021313.
Meibom, A., Cuif, J.-P., Houlbreque, F., Mostefaoui, S., Dauphin, Y., et al., 2008. Chemical variations at ultra-strcutural length-scales in coral skeleton. Geochim. Cosmochim. Acta 72, 1555–1569.
Mischor, B., 1975. Zur Morphologie und Regeneration der Hohlstacheln von *Diadema antillarum* Philippi und *Echinothrix diadema* (L.) (Echinoidea, Diadematidae). Zoomorphologie 82, 243–258.
Okazaki, K., 1960. Skeleton formation of sea urchin larvae. II. Organic matrix of the spicule. Embryologia 5, 283–320.
Politi, Y., Arad, T., Klein, E., Weiner, S., Addadi, L., 2004. Sea urchin spine calcite forms via a transient amorphous calcium carbonate phase. Science 306, 1161–1164.
Reyes-Bermudez, A., Lin, Z., Hayward, D.C., Miller, D.J., Ball, E.E., 2009. Differential expression of three galaxin-related genes during settlement and metamorphosis in the scleractinian coral *Acropora millepora*. BMC Evol. Biol. 9, 178. doi:10.1186/1471-2148-9-178.
Ries, J.B., 2004. Effect of ambient Mg/Ca ratio on Mg fractionation in calcareous marine invertebrates: a record of the oceanic Mg/Ca ratio over the Phanerozoic. Geology 32 (11), 981–984.
Russell, M.P., Urbaniak, L.M., 2004. Does calcein affect estimates of growth rates in sea urchins? In: Heinzeller, Th., Nebelsick, J.H. (Eds.), Echinoderms: München. Taylor & Francis, London, pp. 53–57.
Schöne, B.R., Dunca, E., Fiebig, J., Pfeiffer, M., 2005. Mutvei's solution: an ideal agent for resolving microgrowth structures of biogenic carbonates. Palaeogeogr. Palaeoclimatol. Palaeoecol. 228, 149–166.
Smith, A.B., 1980. Stereom microstructure of the echinoid test. Spec. Paper Palaeont. 25, 1–81.
Stolarski, J., 2003. 3-Dimensional micro- and nanostructural characteristics of the scleractinian corals skeleton: a biocalcification proxy. Acta Palaeontol. Pol. 48, 497–530.
Thébault, J., Chauvaud, L., Clavier, J., Fichez, R., Morize, E., 2006. Evidence of a 2-day periodicity of stria formation in the tropical *Comtopallium* radula using calcien marking. Mar. Biol. 149, 257–267.
Le Tissier, Md'A., 1991. The nature of the skeleton and skeletogenic tissue in the Cnidaria. Hydrobiologia 216 (217), 397–402.
Weiner, S., 1985. Organic matrix-like macromolecules associated with the mineral phase of sea urchin skeletal plates and teeth. J. Exp. Zool. 234, 7–15.
Wilt, F.H., Killian, C.E., Livingston, 2003. Development of calcareous skeletal elements in invertebrates. Differentiation 71, 237–250.
Yang, L., Killian, C.E., Kunz, M., Tamura, N., Gilbert, P.U.P.A., 2011. Biomineral nanoparticles are space-filling. Nanoscale 3, 603–609.